

Physical properties of $\text{Cu/La}_{0.67}\text{Ba}_{0.33}\text{MnO}_3/\text{SrTiO}_3$: Nb junctions with ultrathin manganite layers

This article has been downloaded from IOPscience. Please scroll down to see the full text article.

2011 J. Phys. D: Appl. Phys. 44 025002

(<http://iopscience.iop.org/0022-3727/44/2/025002>)

View [the table of contents for this issue](#), or go to the [journal homepage](#) for more

Download details:

IP Address: 159.226.35.189

The article was downloaded on 10/01/2011 at 06:42

Please note that [terms and conditions apply](#).

Physical properties of Cu/La_{0.67}Ba_{0.33}MnO₃/SrTiO₃:Nb junctions with ultrathin manganite layers

Weiwei Gao¹, Xuan Sun², Baogen Shen¹ and Jirong Sun¹

¹ Beijing National Laboratory for Condensed Matter Physics and the Institute of Physics, Chinese Academy of Sciences, Beijing 100190, People's Republic of China

² Department of Physics, Beihang University, Beijing 100080, People's Republic of China

E-mail: jrsun@g203.iphy.ac.cn

Received 19 September 2010, in final form 17 November 2010

Published 16 December 2010

Online at stacks.iop.org/JPhysD/44/025002

Abstract

We performed a systematic study on a Cu/La_{0.67}Ba_{0.33}MnO₃/SrTiO₃:Nb (Cu/LBMO/STON) junction with a manganite layer, a few unit cells in width, focusing on the evolution of Cu–STON coupling as the film thickness of LBMO grew. The physical properties of the junction are found to be jointly determined by the electrode, the film and the substrate when the film thickness of LBMO is below ~ 1 nm, with a carrier tunnelling process and a weakly rectifying feature. A LBMO film above ~ 1 nm completely screens the electrode–substrate interaction, enhancing the rectifying character of the junctions significantly. A further increase in film thickness leads only to a minor modification of the junctions.

(Some figures in this article are in colour only in the electronic version)

1. Introduction

A manganite-based junction is the simplest manganite heterostructure. Since its first occurrence [1], much effort has been devoted to the exploration of the effects that are absent in conventional junctions and, indeed, distinctive phenomena such as magnetic field-dependent rectifying characteristics and photovoltaic effect have been observed [2–4]. Intensive work has also been undertaken to modify the interfacial structure, and the remarkable effects caused by interfacial decorations, such as the two-process-featured rectifying behaviour in La_{0.67}Ca_{0.33}MnO₃/LaMnO₃/SrTiO₃:Nb junctions [5] and the growth of interfacial potential after the introduction of a SrMnO₃ monolayer in La_{0.7}Sr_{0.3}MnO₃/SrTiO₃:Nb junctions [6], have been detected.

As well documented, the physical properties of a heterostructure are determined mainly by the interface. However, the atomic and electronic environment at the interface could be considerably different from that of the interior. Based on an *in situ* photoemission experiment, Minohara *et al* [7] have studied the band structure of SrTiO₃:Nb as a La_{0.6}Sr_{0.4}MnO₃ film was deposited layer by layer, and observed a gradual development of band bending.

The minimal layer thickness for a saturated band bending is ~ 1.2 nm, which is also the depletion width in La_{0.6}Sr_{0.4}MnO₃. A thorough understanding of the interfacial processes is therefore particularly important for manganite engineering. There are also distinctive issues for ultrathin film junctions, such as the effects of electrode–substrate coupling and finite size due to the comparability of layer thickness and depletion width. The evolution of physical properties of the junctions as film thickness reduces can provide valuable information about the interface, especially when the film width is only a few unit cells. In this paper, we performed a systematic study on a Cu/La_{0.67}Ba_{0.33}MnO₃/SrTiO₃:Nb (Cu/LBMO/STON) junction with a manganite layer, a few unit cells in width. Special attention has been paid to the evolution of the rectifying behaviours of the junctions as film thickness varies, particularly the variation of Cu–STON coupling. The physical properties of the junction are found to be jointly determined by the electrode, the film and the substrate when the LBMO thickness is below ~ 2 unit cells, with a quantum tunnelling process and weakly rectifying character. In contrast, a LBMO film above 2 unit cells completely screens the electrode–substrate interaction, enhancing the rectifying character of the junction significantly.

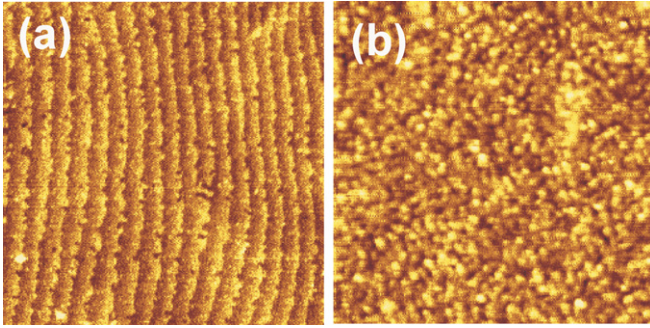


Figure 1. Topology of the LBMO films with thicknesses of 0.5 nm (a) and 15 nm (b). The size of the image is $1 \times 1 \mu\text{m}^2$.

2. Experiments

A series of manganite junctions were fabricated by growing, via the pulsed laser ablation technique, $\text{La}_{0.67}\text{Ba}_{0.33}\text{MnO}_3$ (LBMO) films on (001)-orientated $\text{SrTiO}_3:0.05 \text{ wt\% Nb}$ (STON) substrates of dimension $3 \times 1 \text{ mm}^2$. The substrates were prior treated at a temperature of $\sim 720^\circ\text{C}$ for $\sim 20 \text{ min}$ in an atmosphere of $\sim 10^{-5} \text{ Pa}$ to obtain a flat surface characterized by terrace steps. LBMO was chosen because of its small lattice mismatch with the substrate (less than 0.15%). In the deposition process, the temperature of the substrate was kept at 720°C , and the oxygen pressure at $\sim 60 \text{ Pa}$. The film thicknesses were $t = 0, 0.5, 1, 2, 4, 6, 15$ and 30 nm , controlled by deposition time. The deposition rate was $\sim 0.3 \text{ \AA s}^{-1}$, which was carefully calibrated to guarantee the accuracy of the film thickness. As electrodes, two copper pads of size $1 \times 1 \text{ mm}^2$ were deposited on the manganite films and STON, respectively. Appropriate electric pulses were applied to the bottom Cu–STON contact to break the possible Schottky barrier and get an Ohmic contact. The resistances were $\sim 15 \Omega$ and $\sim 50 \Omega$ for the Cu–STON and Cu–LBMO contacts, respectively.

3. Results and discussion

Figure 1 shows the atomic force microscope (AFM) image of the typical LBMO films. Terrace-featured topology is observed in the films below 1 nm, and the terrace step is uniform, $\sim 0.4 \text{ nm}$, across the region studied, which is an indication of layer-by-layer film growth. The terrace structure becomes vague above a thickness of 2 nm, and a morphology characterized by densely packed grains appears. The root mean square roughness varies between ~ 0.2 and $\sim 0.3 \text{ nm}$ as the film thickness grows. The relatively high oxygen pressure affects the growth mode of the LBMO films.

Figure 2 shows the current density (J)–voltage (V) characteristics of the Cu/LBMO(t)/STON junctions of $t = 0, 0.5, 1$ and 6 nm , recorded at a fixed temperature of 290 K . Cu/STON is weakly asymmetric against polarity. However, the junction with a LBMO layer above 1 nm is strongly rectifying, and the rectifying ratio is, for example, greater than $\sim 3 \times 10^3$ at a bias of 0.3 V . The junction resistances, in the zero-bias limit, are $\sim 1 \times 10^3 \Omega$, $\sim 1.2 \times 10^4 \Omega$ and $\sim 3 \times 10^5 \Omega$ for film thicknesses of 0 nm , 0.5 nm and 1 nm , respectively, and above $10^6 \Omega$ for other junctions (junction area

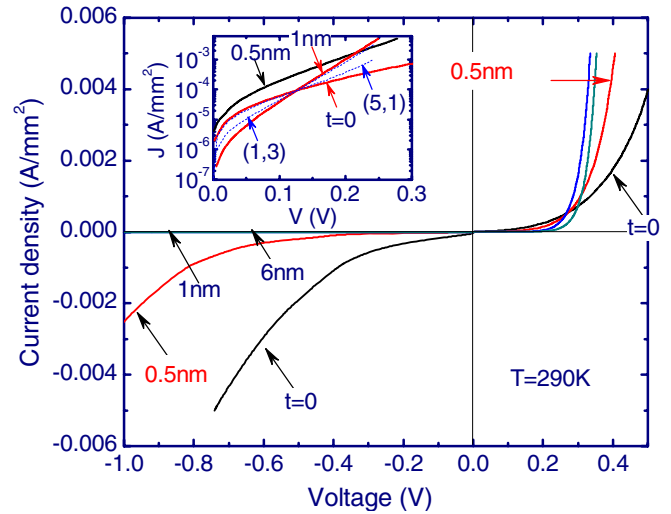


Figure 2. Current density–voltage characteristics of LBMO/STON with film thicknesses of $t = 0, 0.5, 1$ and 6 nm , measured at a fixed temperature of 290 K . Inset plot shows the comparison of the observed (solid lines) and calculated (dashed lines) J – V curves. The parameters used in the calculation are $(\alpha, \beta) = (1, 3)$ and $(5, 1)$, as marked in the figure.

$= 1 \times 1 \text{ mm}^2$). The work function/electron affinity values of Cu, LBMO and STON are $\sim 4.6 \text{ eV}$, $\sim 4.9 \text{ eV}$ and $\sim 3.9 \text{ eV}$ [8], respectively. This implies a slightly lower interfacial barrier in Cu/STON, which is consistent with the low resistance of this junction. With the incorporation of the LBMO layer, the junction resistance grows rapidly, and reaches nearly the maximal value at a film thickness of 1 nm .

It would be instructive to perform a quantitative analysis of the $\ln(J) - \ln[\exp(eV/nk_B T) - 1]$ relations of the junctions, where e is the electron charge and n the ideality factor. As shown in figure 3(a), two visible physical processes (marked by labels LV and HV) linked by an electronic transition can be reorganized for the Cu/STON junction. The saturation current is different for these two states, low for the low-bias state and high for the high-bias state. These are typical features of the Cu/STON junction. Of special interest is the 0.5 nm junction (figure 3(b)). Although the electronic transition is significantly weakened, the similarity of the J – V characteristics of this junction to those of Cu/STON can still be recognized. This implies an electronic coupling between Cu and STON through the intermediate LBMO layer. However, the LBMO layer does modify the J – V characteristics considerably, and a layer of 1 nm completely screens the Cu–STON interaction (figures 3(c) and (d)).

Based on the analysis of the $\ln(J) - \ln[\exp(eV/nk_B T) - 1]$ relations, the ideality factor of the junctions can be obtained. It is considerably large for the junction of $t = 0$, ~ 4.4 at 330 K and ~ 11.8 at 110 K . A quantitative analysis leads to a simple relation: $1/n \approx 0.009 + 0.0007T$, marked by the solid curve (dark blue) in the inset plot in figure 3(a). With the incorporation of a 0.5 nm LBMO layer, n decreases, and its temperature dependence becomes $1/n \approx -0.01 + 0.0015T$. A common feature of the n – T relations for $t = 0$ and 0.5 nm is the reverse dependence on temperature. According to the semiconductor theory, there are two factors that can affect the

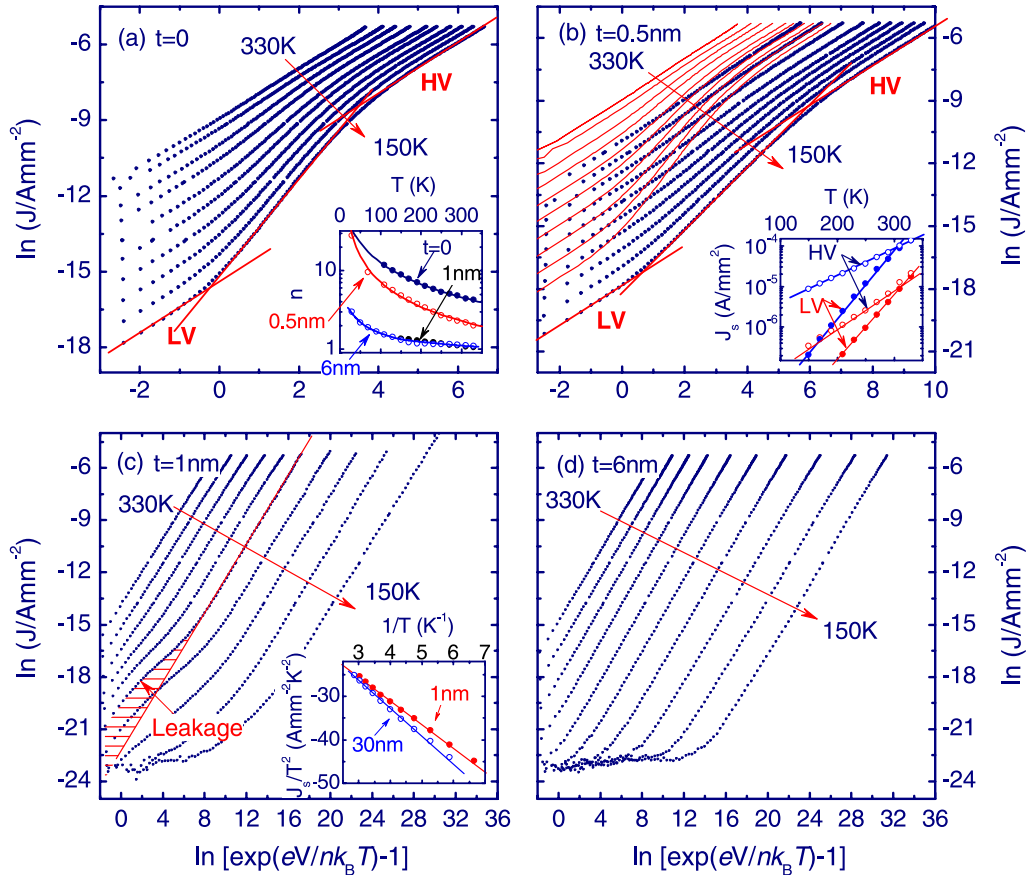


Figure 3. $\ln(J)-\ln[\exp(eV/nk_B T) - 1]$ relations of LBMO/STON with film thicknesses of 0 (a), 0.5 (b), 1 (c) and 6 nm (d), measured in the temperature range from 150 to 330 K with a temperature step of 20 K. The data for $t = 0$ are also shown in (b) as solid curves for comparison. The shaded area in (c) marks the deviation from linearity due to the electric leakage. Inset plot in (a) shows the ideality factor of the junctions. Solid curves for $t = 0$ and 0.5 nm are calculated results (see the text). Inset plot in (b) shows saturation currents as functions of temperature for the junction of $t = 0$ (blue symbols) and 0.5 nm (red symbols). LV and HV mark the low- and high-bias processes, respectively. Inset plot in (c) displays the saturation current–reciprocal temperature relation for the junctions of 1 and 30 nm. Solid lines are guides for the eye.

ideality factor. The first one is the inhomogeneous junction interface and the second one is the leakage current. The latter could be the main reason for the unusual ideality factor of the present junction. In fact, the $1/T$ dependence of n for $t = 0.5$ nm indicates the temperature independence of the $\ln(J)-V$ slope, which is a signature of electron/hole tunnelling across the depletion layer [9]. It is possible that a LBMO film of 0.5 nm cannot build up an interfacial barrier thick enough to prevent carrier tunnelling.

The transport mechanism can be elucidated by the analysis of the J_s-T relation. As well established, the saturation current will vary following the relations of $J_s \propto \exp(aT)[\propto \exp(-\Phi_B/k_B T)]$ for the tunnelling (thermionic) process, where a is an appropriate constant and Φ_B the interfacial barrier [9, 10]. In the inset plot in figure 3(b) we show the saturation current as a function of temperature for the two processes in the Cu/STON and LBMO(0.5 nm)/STON junctions. Well-linear $\ln(J_s)-T$ relations are observed, and the $\ln(J_s)-T$ slopes are ~ 0.038 and ~ 0.022 $\ln(\text{A}/\text{mm}^2)/\text{K}$ for the low- and high-bias processes, respectively, for the Cu/LBMO/STON junction.

For the junctions of $t \geq 1$ nm, the $\ln(J)-\ln[\exp(eV/nk_B T) - 1]$ curves recorded at different temperatures are well linear, downwards shifting upon cooling. The

former is a character of thermionic emission process and the latter is a consequence of saturation current depression. Although the film thickness is slightly increased, the effect of temperature on the ideality factor is considerably suppressed. It is, for example, for the junction of $t = 1$ nm, ~ 1.1 at $T = 330$ K and ~ 2 at $T = 50$ K. It is interesting to note that all the junctions of $t \geq 1$ nm exhibit essentially identical ideality factors. This could be an indication of the establishment of a mature interface state above 1 nm. A further analysis indicates the presence of a linear relation between $\ln(J_s)$ and $1/T$, a typical feature of thermionic process (inset in figure 3(c)). The interfacial barriers determined by the $\ln(J_s)-1/T$ slopes are similar, ~ 0.46 eV for $t = 1$ nm, ~ 0.58 eV for $t = 6$ nm and ~ 0.53 eV for $t = 30$ nm. The sudden change in the $J-V$ characteristics of the junction when the film thickness increases from $t = 0.5$ to 1 nm suggests the presence of a critical film thickness, which is between 0.5 and 1 nm, for the screening of Cu-STON coupling.

Figure 4 is a summary of the junction resistance, ideality factor, rectifying ratio and interfacial barrier of LBMO(t)/STON as functions of film thickness, acquired at a selected temperature of 290 K. All of the quantities, except the interfacial barrier, experience a sudden jump as t grows from

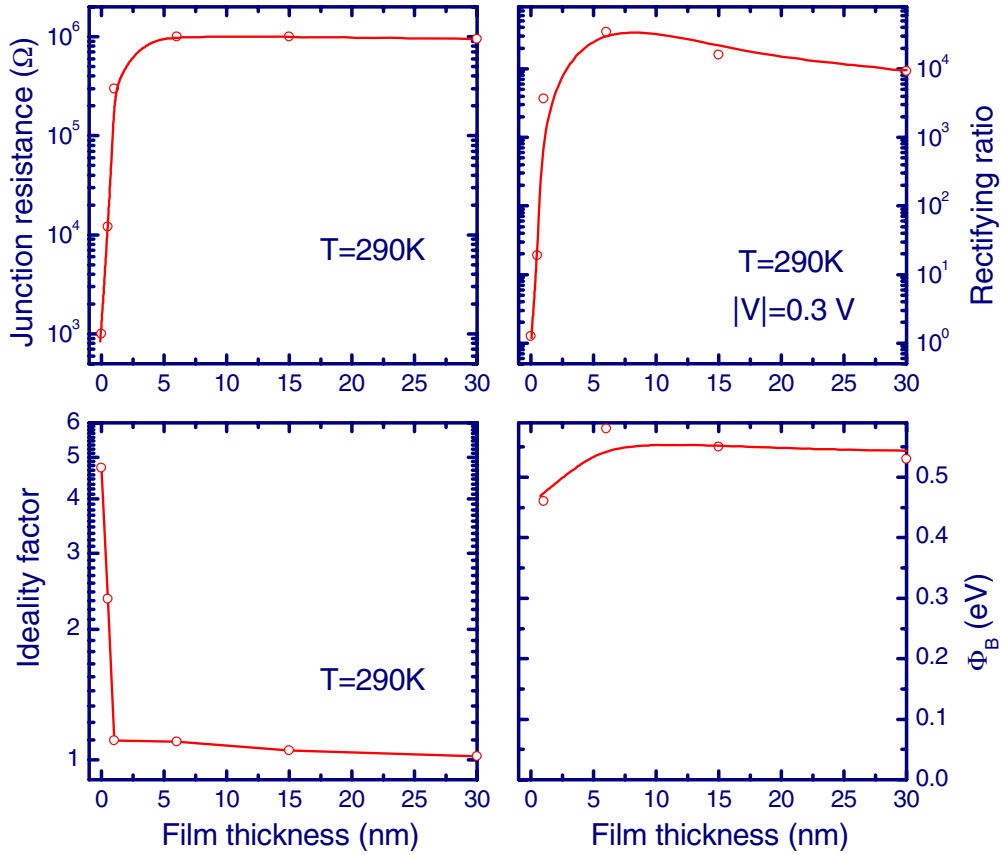


Figure 4. Junction resistance, ideality factor, rectifying ratio and interfacial barrier of LBMO/STON as functions of film thickness, acquired at a selected temperature of 290 K.

0 to 1 nm. The interfacial barrier of the junction of $t = 0$ and 0.5 nm cannot be determined based on the J - V curve analysis because of the severe leakage current. However, Φ_B remains essentially unchanged above $t = 1$ nm. It is therefore clear that the threshold film thickness that screens the Cu-STON interaction is ~ 1 nm.

One may argue that a layer of 0.5 nm cannot guarantee a complete coverage of the substrate and, as a result, the J - V characteristics could be jointly determined by the Cu/STON and LBMO/STON junctions. In the case of partial substrate coverage, the J - V relations of the junctions could be simulated by $J(V) = [\alpha J_1(V) + \beta J_2(V)]/(\alpha + \beta)$, where $J_1(V)$ and $J_2(V)$ are the characteristics of the Cu/STON and LBMO(1 nm)/STON junctions, respectively, noting that the J - V curves are essentially unchanged above 1 nm. However, we failed to reproduce the characteristics of LBMO(0.5 nm)/STON by simply adjusting α and β . These results suggest that the film discontinuity may not be the main origin of the abnormal behaviour. The inset in figure 2 shows the observed J - V curves for $t = 0$ nm, 0.5 nm and 1 nm and the calculated results for $t = 0.5$ nm, adopting the parameters of $(\alpha, \beta) = (1, 3)$ and $(5, 1)$, respectively, at a selected temperature of 290 K.

The LBMO layer, though it is thin, will cause a band bending of STON, and thus affect the interfacial barrier. This is the apparent explanation for the considerable difference in the J - V characteristics of Cu/STON and LBMO(0.5 nm)/STON. However, LBMO(0.5 nm)/STON is also obviously different

from the LBMO(t)/STON of $t \geq 1$ nm. Because of the dominant role of surface states on the electronic structure, the work function of the LBMO (0.5 nm) layer could be different from that of the bulk LBMO. When it is lower than or similar to that of Cu, the interfacial barrier will be determined mainly by Cu and STON. A LBMO layer of 0.5 nm is actually transparent to charge carriers, and will not prevent the charge exchange between Cu and STON. As a consequence, the rectifying behaviour of LBMO(0.5 nm)/STON is jointly determined by Cu, LBMO and STON. This result indicates that the effects of electrodes must be taken into consideration for the ultrathin film junction. Another remarkable observation of this work is that the LBMO layer of 1 nm completely screens the Cu-STON coupling. Although this layer could also be transparent to charge carriers, it builds up an interfacial barrier at the LBMO/STON interface that prevents further diffusion of the charge carriers from Cu into STON. An inference from the present result is that the LBMO film of 1 nm exhibits the electronic structure that is not very much different from the bulk. The complex behaviour of Cu/STON is also interesting. It could be a topic of further studies.

4. Summary

We performed a systematic study on a Cu/La_{0.67}Ba_{0.33}MnO₃/SrTiO₃:Nb (Cu/LBMO/STON) junction with a manganite layer, a few unit cells in width, focusing on the evolution of Cu-STON coupling as the film thickness of LBMO grew.

The physical properties of the junction are found to be jointly determined by the electrode, the film and the substrate when the film thickness of LBMO is below ~ 1 nm, with a carrier tunnelling process and weakly rectifying feature. A LBMO film above ~ 1 nm completely screens the electrode–substrate interaction, enhancing the rectifying character of the junctions significantly. A further increase in film thickness leads only to a minor modification of the junctions. It is therefore clear that the effects of electrode should be considered when artificial oxide structures based on ultrathin layers are designed.

Acknowledgments

This work has been supported by the National Basic Research of China, the National Natural Science Foundation of China, the Knowledge Innovation Project of the Chinese Academy of Science and the Beijing Municipal Nature Science Foundation.

References

- [1] Sugiura M, Uragou K, Noda M, Tachiki M and Kobayashi T 1999 *Japan. J. Appl. Phys. Part 1* **38** 2675
- [2] Tanaka H, Zhang J and Kawai T 2001 *Phys. Rev. Lett.* **88** 027204
Sun J R, Xiong C M, Zhao T Y, Zhang S Y, Chen Y F and Shen B G 2004 *Appl. Phys. Lett.* **84** 1528
Nakagawa N, Asai M, Mukunoki Y, Susaki T and Hwang H Y 2005 *Appl. Phys. Lett.* **86** 082504
- [3] Sun J R, Shen B G, Sheng Z G and Sun Y P 2004 *Appl. Phys. Lett.* **85** 3375
Sheng Z G, Zhao B C, Song W H, Sun Y P, Sun J R and Shen B G 2005 *Appl. Phys. Lett.* **87** 242501
- [4] Muramatsu T, Muraoka Y, Yamauchi T, Yamaura J and Hiroi Z 2004 *J. Magn. Magn. Mater.* **272–276** E787
- [5] Lv W M, Wei A D, Sun J R, Chen Y Z and Shen B G 2009 *Appl. Phys. Lett.* **94** 082506
- [6] Hikita Y, Nishikawa M, Yajima T and Hwang H Y 2009 *Phys. Rev. B* **79** 073101
- [7] Minohara M, Furukawa Y, Yasuhara R, Kumigashira H and Oshima M 2009 *Appl. Phys. Lett.* **94** 242106
- [8] Reagor D W, Lee S Y, Li Y and Jia Q X 2004 *J. Appl. Phys.* **95** 7971
Robertson J 2000 *J. Vac. Sci. Technol. B* **18** 1785
- [9] Sharma B L and Purohit R K 1974 *Semiconductor Heterojunctions* (Oxford: Pergamon) pp 1–13
- [10] Sze S M 1981 *Physics of Semiconductor Devices* 2nd edn (New York: Wiley)